Structure and Energetics of Azobenzene on Ag(111): Benchmarking Semiempirical Dispersion Correction Approaches

G. Mercurio,[1,2] E. R. McNellis,[3] I. Martin,[4] S. Hagen,[4] F. Leyssner,[4] S. Soubatch,[1,2] J. Meyer,[3] M. Wolf,[3,4] P. Tegeder,[4] F. S. Tautz,[1,2,*] and K. Reuter[3]

[1]*Institut für Bio- und Nanosysteme 3, Forschungszentrum Jülich, 52425 Jülich, Germany*
[2]*JARA-Fundamentals of Future Information Technology*
[3]*Fritz-Haber-Institut der Max-Planck-Gesellschaft, Faradayweg 4-6, 14195 Berlin, Germany*
[4]*Fachbereich Physik, Freie Universität Berlin, Arnimallee 14, 14195 Berlin, Germany*

(Received 27 August 2009; published 19 January 2010)

We employ normal-incidence x-ray standing wave and temperature programed desorption spectroscopy to derive the adsorption geometry and energetics of the prototypical molecular switch azobenzene at Ag(111). This allows us to assess the accuracy of semiempirical correction schemes as a computationally efficient means to overcome the deficiency of semilocal density-functional theory with respect to long-range van der Waals (vdW) interactions. The obtained agreement underscores the significant improvement provided by the account of vdW interactions, with remaining differences mainly attributed to the neglect of electronic screening at the metallic surface.

DOI: 10.1103/PhysRevLett.104.036102 PACS numbers: 68.43.Bc, 68.43.Vx, 68.49.Uv

The potential of a future molecular nanotechnology has motivated many studies of functional organic molecules at metal surfaces. In this context, a simulation platform which allows the precise prediction of all relevant modes of the molecule-substrate interaction (chemical bonds of specific groups, Pauli repulsion, steric hindrance, and dispersion interaction) is required. Here, the adsorption of organic molecules with highly polarizable conjugated ring systems on metals poses particular difficulties to theory, because the prevalence of dispersive van der Waals (vdW) interactions restricts the applicability of semilocal exchange and correlation (xc) functionals within density-functional theory (DFT). Since high-level theories that include nonlocal vdW interactions by construction are still barely tractable for large surface-adsorbed molecules, computationally inexpensive semiempirical dispersion correction schemes to semilocal DFT (DFT-D) represent an appealing alternative [1–7]. In these approaches, vdW interactions are considered approximately by adding a pairwise interatomic C_6R^{-6} term to the DFT energy. At distances below a cutoff, motivated by the vdW radii of the atom pair, this long-range dispersion contribution is heuristically reduced to zero by multiplication with a short-range damping function.

While of proven accuracy for a range of molecular systems [2,3,6], the applicability of the DFT-D approach to organic molecules *adsorbed at metal surfaces* is uncertain. First, it is not clear how the results are affected by the neglected fact that the dispersive interaction between the adsorbate and more distant substrate atoms is screened by the intervening metal layers. Second, adsorbate molecules which also interact covalently with the substrate exhibit molecule-substrate bond distances that are so short that the uncertainties in the heuristic damping function of the dispersion term mingle in an uncontrolled way with deficiencies of the employed semilocal DFT xc functional. In this situation, accurate data from experiment for mindfully chosen prototype molecules provide a reference to judge whether the improvements brought by including long-range vdW interactions semiempirically outweigh the above mentioned shortcomings.

In this Letter, we respond to this need by providing reference data for the molecular switch azobenzene (C_6H_5-N = N-C_6H_5) at Ag(111). In particular, we have used the normal-incidence x-ray standing wave technique (NIXSW) to determine key structural parameters of adsorbed azobenzene and temperature programed desorption (TPD) for measuring its adsorption energy. Compared to this reference data, we find that recent DFT-D schemes predict structural properties rather accurately but lead to a sizeable overbinding. We attribute this surprising inconsistency between the simulated structure and the corresponding adsorption energy primarily to the neglect of electronic screening at the metal surface. Indeed, already a crude account of the latter brings also the calculated binding energy close to the measured value.

We start with a qualitative discussion of the anticipated azobenzene-surface interaction, which is characterized by a balance between four major contributions: a covalent bond between the azobridge ($-$ N = N $-$) and Ag(111), the vdW attraction between the metal and the phenyl rings, the energetic penalty due to the distortion of the gas phase molecular geometry, and the Pauli repulsion between the phenyl rings and the substrate. In the flat adsorption geometry of the more stable *trans* isomer of azobenzene [Fig. 1(a)], the first and last contributions compete with each other, since the formation of covalent N-Ag bonds requires a short $d_{\text{N-Ag}}$ distance at which the phenyl rings may already experience a substantial Pauli repulsion, leading to a butterflylike configuration with a finite tilt angle $\tilde{\omega}$

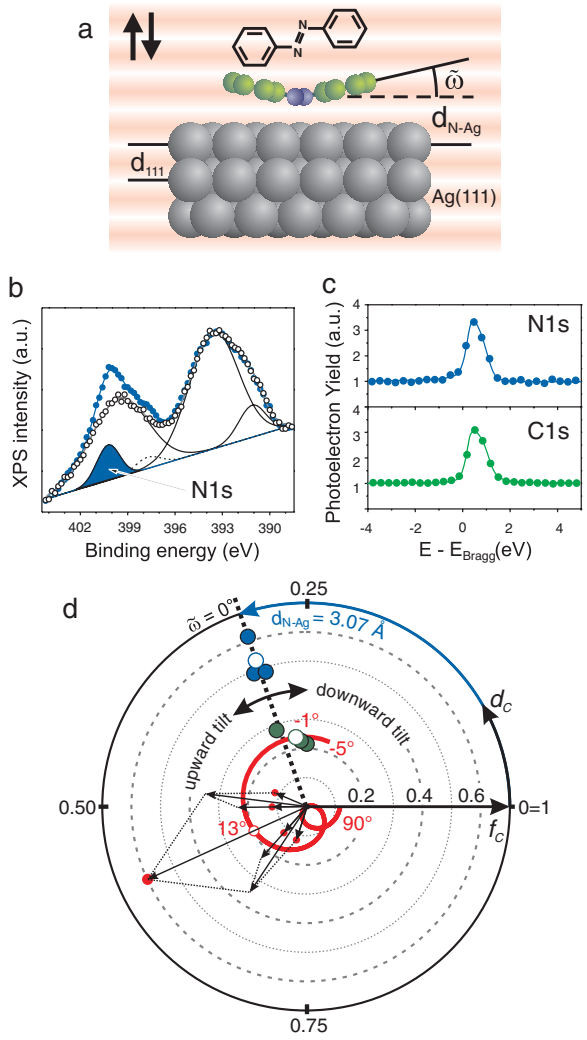

FIG. 1 (color). (a) Structure formula of azobenzene and schematic adsorption model in a butterfly geometry (side view) with key structural parameters $\tilde{\omega}$ and $d_{\text{N-Ag}}$ (see text). (b) Experimental photoemission spectra of azobenzene/Ag(111) (blue ●) and clean Ag(111) (○). For azobenzene/Ag(111), the corresponding fit is also displayed (blue solid line). For clean Ag(111), the three component lines of the fit are plotted as solid black lines. The fit of azobenzene/Ag(111) requires two additional components, one of them shaded in blue (N1s) and the other displayed as a dashed line (see text). (c) Extracted PEY curves as a function of photon energy relative to the Bragg energy (2.635 keV, ●) and the corresponding fits (solid lines) [12]. Each curve is an average of three NIXSW data sets taken at different positions on the crystal. (d) Argand diagram of d_c and f_c for N1s (blue ●) and C1s (green ●), and corresponding average points (○). The red spiral represents calculated d_c and f_c for C1s as $\tilde{\omega}$ sweeps from $-5°$ to 90°. The vector sum of the six phenyl C atoms that contribute to this is illustrated in the bottom left part (zoomed by a factor of 3) for $\tilde{\omega} = 13°$.

[cf. Fig. 1(a)]. Note, however, that attractive vdW interactions have the tendency to pull the molecule and, in particular, the phenyl rings further to the surface, thereby potentially decreasing both $d_{\text{N-Ag}}$ and $\tilde{\omega}$. Together with the adsorption energy, these two structural parameters are therefore sensitive gauges of the balance between the covalent N-Ag and dispersive phenyl-substrate interactions and hence constitute a challenging test for any simulation platform aiming at a faithful description of the role of dispersion forces in the adsorption of aromatic molecules.

NIXSW yields accurate values for adsorption heights and adsorption-induced molecular distortions [8–11]. However, using conventional data analysis techniques, it is difficult to differentiate between the positions of identical species with small chemical core level shifts, such as the various carbon atoms in the phenyl rings of azobenzene. Employing a novel analysis scheme, we are able to overcome this difficulty and extract $\tilde{\omega}$ from a *single* measured parameter averaged over all carbon atoms in azobenzene if $d_{\text{N-Ag}}$ is also known; the latter is measured straightforwardly in NIXSW. In short, the NIXSW technique exploits the fact that adsorbate atoms located at the positions of the antinode planes of a standing x-ray wave field induced by Bragg-reflection exhibit a maximum in the photoelectron yield (PEY). Scanning the photon energy through the Bragg energy shifts the position of the antinodes from the lattice planes to halfway positions between them. At different photon energies, the PEY thus probes different vertical locations of adsorbate atoms relative to the substrate lattice planes and can be used to extract element-specific adsorption heights.

The NIXSW experiments have been conducted at the beam line ID32 of the European Synchrotron Radiation Facility on a monolayer (ML) of azobenzene on Ag(111). The measured PEY curves (i.e., integrated photoemission peak intensities versus photon energy) for N1s and C1s core levels were fitted using the program DARE [12]. The fits provide two structural parameters for each species: the coherent position d_c and the coherent fraction f_c. The former is related to the average distance of the photoemitter from the relevant family of bulk lattice planes; the latter describes its actual distribution. For C, the fits displayed in Fig. 1(c) yield $d_c = 0.28 \pm 0.03$ and $f_c = 0.24 \pm 0.04$. To quantify the N1s PEY at Ag(111), the N1s core level must be separated from plasmonic Ag3d satellites. For clean Ag(111), these satellites are shown as open circles in Fig. 1(b). They can be deconvoluted into three components. After the deposition of azobenzene, two additional components appear in Fig. 1(b). Because of the symmetry of the molecule and its adsorption site on the Ag(111) surface, a common N1s component is expected for both N atoms; hence the second new component is assigned to adsorbate-induced changes to the plasmonic satellites. Indeed, NIXSW shows that the line at 397.8 eV follows the substrate ($d_c \approx 1$). The fits of the PEY curve for N1s at 400.2 eV give an average $d_c = 0.30 \pm 0.01$ and $f_c = 0.53 \pm 0.09$ [Fig. 1(c)]. This yields $d_{\text{N-Ag}} = 3.07 \pm 0.02$ Å as our first key structural parameter.

To analyze the internal geometry of the adsorbed azobenzene molecule, i.e., $\tilde{\omega}$, we discuss the NIXSW results in terms of an Argand diagram [Fig. 1(d)], a polar plot in

which f_c is the radius vector and d_c is proportional to the polar angle, with $d_c = 0$ and $d_c = 1$ corresponding to 0° and 360°, respectively. In this diagram, the contributions of atoms that belong to the same species but are located at different heights to the overall (measured) d_c and f_c can be expressed as a vector sum. An example is shown in the lower left-hand portion of Fig. 1(d) for the case of $\tilde{\omega} = 13°$, with the height of the azobridge fixed to the experimentally determined value of $d_{\text{N-Ag}}$. The red spiral then indicates how the C sum vector behaves if $\tilde{\omega}$ is changed from −5° to 90°. Comparison to the actually measured values, i.e., the intersection of the spiral with the averaged experimental (d_c, f_c) point for C, uniquely determines the phenyl tilt angle as $-1 \pm 1.5°$ [13].

With the key structural parameters determined, we proceed to the TPD experiments. Figure 2 shows desorption spectra as a function of coverage in the submonolayer regime where only one desorption peak is observed. With increasing coverage θ, this peak broadens and shifts towards lower temperatures, as has also been observed for other azobenzene derivatives on noble metal surfaces [14]. In order to derive the activation energy for desorption E_{des}, we utilize the so-called complete analysis [15]. In this method plots of the logarithm of the desorption rate $[\ln(d\theta/dt)]$ versus the reciprocal temperature at different relative coverages provide E_{des} from the slope of the lines as exemplified in the inset of Fig. 2. In the low-coverage regime $\theta \leq 0.3$ ML, we determine a nearly constant desorption energy of $E_{\text{des}} = 1.00 \pm 0.1$ eV.

We now compare the experimental data to the results obtained with the recent DFT-D schemes due to Grimme (G06) [3] and Tkatchenko and Scheffler (TS) [6]. In Fig. 3, the zero-point energy (ZPE) corrected E_{des}, calculated at the most stable lateral adsorption site [7], are displayed versus $d_{\text{N-Ag}}$. The calculations have been performed with a locally modified version of the CASTEP code [16], using the semilocal PBE xc functional [17] and the same computational setup as detailed in Ref. [7]. At the optimized adsorption heights, both bare DFT-PBE and the two DFT-D schemes yield an essentially planar molecule, with tilt angles of $\tilde{\omega}_{\text{PBE}} = +1°$, $\tilde{\omega}_{\text{PBE+G06}} = +1°$, and $\tilde{\omega}_{\text{PBE+TS}} = +3°$, all of them in similar agreement with the experimental value. This small variation indicates that, irrespective of the dispersion interaction, the differential surface interaction within the extended molecule (i.e., the difference between the surface interactions of the various parts of the molecule) is too weak to overcome the molecular distortion cost. In contrast, the adsorption height $d_{\text{N-Ag}}$ is a very sensitive indicator of the strength of vdW interactions. Compared to the experimental reference, bare DFT-PBE strongly overestimates this distance (3.64 Å) and produces only a weak binding. This is a direct consequence of the failure of the semilocal xc functional to account for the long-range dispersive interactions and has, e.g., similarly been observed for PTCDA/Ag(111) [8]. Instead, both G06 and TS lead to a sizable reduction of $d_{\text{N-Ag}}$ to 2.75 Å and 2.98 Å, respectively, with the latter in good agreement with experiment.

Unfortunately, the improved structure goes hand in hand with a notable overbinding. In fact, the popular G06 scheme (2.16 eV) overbinds more than bare DFT-PBE underbinds. The refined TS scheme with its account for the variation of dispersion coefficients in differently bonded atoms performs somewhat better (1.71 eV), in

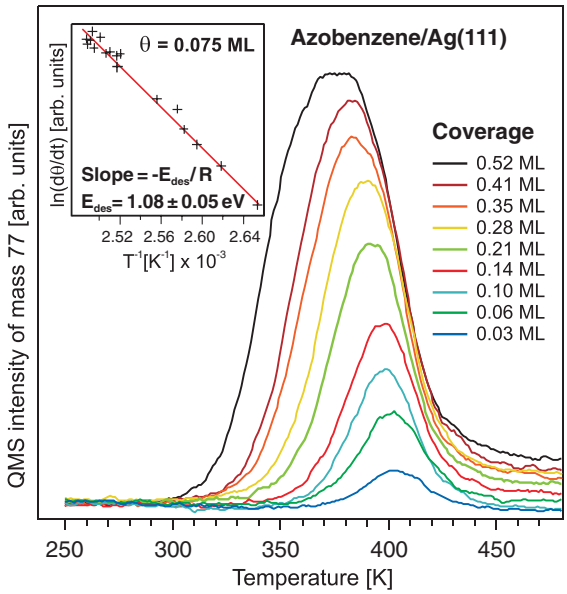

FIG. 2 (color). Thermal desorption spectra at different relative coverages θ in ML recorded with a linear heating rate of 1 K/s at the fragment mass of 77 amu ($C_6H_5^+$). 1 ML is defined as the coverage corresponding to the saturated desorption peak. The inset plots the desorption rate $\ln(d\theta/dt)$ against the reciprocal temperature at $\theta = 0.075$ ML. The slope of the line, $-E_{\text{des}}/R$ with R the gas constant, then determines the activation energy for desorption at this coverage, here $E_{\text{des}}(0.075\ \text{ML}) = 1.08 \pm 0.05$ eV.

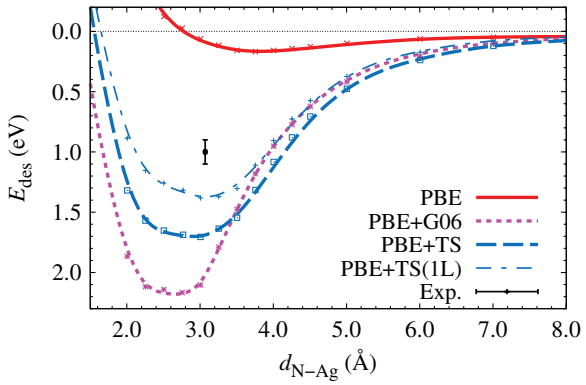

FIG. 3 (color). ZPE-corrected desorption energy curves, computed with bare DFT-PBE and the two discussed DFT-D schemes. The black data point marks the experimental values and errors. Also shown is the curve computed with the TS correction reduced to the topmost layer Ag atoms (see text).

agreement with the tendencies observed in molecular systems [6]. If the steepness of the Fermi-type damping function is varied in large bounds, the results of both DFT-D schemes change negligibly, again consistent with previous experience [3,6]. This makes it unlikely that the *functional form* of the damping function itself is responsible for the overbinding. To test whether it might be the *onset* of the damping which is at fault, we verified that the changes introduced upon variations of the approximate vdW radii (which determine this onset) are intuitive: larger cutoff radii lead to less attraction and shift the molecule further away from the surface. Changing the cutoffs therefore *can* reduce the binding energy, but only in conjunction with an increased molecular adsorption height; because the latter is predicted nearly correct by TS, we conclude that its overbinding is *not* related to the employed cutoffs. Very likely, a similar relation between bond strength and adsorption height will also hold for changes of the short-range potential. Shortcomings of the xc treatment by the semilocal PBE functional are therefore also an unlikely cause for the overbinding.

This leads us to conjecture that the main source of the error in the predicted binding energies lies in the *screening* of dispersive attractions between the adsorbate atoms and the increasing number of more distant substrate atoms. By construction, such screening is not accounted for in the strictly pairwise evaluation of the dispersion interaction as inspired by Hamaker theory. Its anticipated effect, however, would primarily be a geometry-unspecific lowering of the overall binding energy. We have mimicked this by reducing the number of substrate layers considered in the pairwise interaction $C_6 R^{-6}$ term and by even diminishing the C_6 coefficients of the Ag atoms in the topmost surface layer; this indeed shifts the computed binding energy curves in Fig. 3 up, but essentially without affecting the position of their minima. Considering that the screening length in Ag is of the order of the interlayer distance, such a restriction of the considered terms to just the topmost layer is justified as a first step to improve the applicability of existing DFT-D schemes to adsorption at metal surfaces. The corresponding curve for the TS scheme (Fig. 3) comes indeed remarkably close to the experimental reference. We have tested both the TS scheme itself and the conjecture that as such it overestimates the binding energies by neglect of screening in calculations for a second adsorbate, PTCDA/Ag(111). We indeed find that restricting the number of substrate layers in the TS scheme again lowers the binding energy without affecting the adsorption height. Just as in the azobenzene case, one-layer restricted TS then yields an adsorption height and binding energy in close agreement with experiment [8] and high-level theory [random phase approximation (RPA)] [18].

In conclusion, we have used detailed structural and energetic data from NIXSW and TPD measurements on azobenzene/Ag(111) to assess the performance of two DFT-D schemes. The most recent TS scheme [6] is found to provide quite accurate structural properties, albeit at a rather sizable overbinding of 0.7 eV. Our analysis relates such a geometry-unspecific overbinding primarily to the neglect of metallic screening of the dispersive interactions. This affirms that existing DFT-D schemes are not suitable to describe the role of vdW interactions in adsorption at metal surfaces comprehensively. However, the insight that the adsorption geometries are less sensitive to the neglect of screening is intriguing. It suggests that these schemes may provide significantly improved structural data at zero additional computational cost. Such structures are then a useful starting point for higher-level first-principles theory, aimed either at refined binding energies or a more comprehensive understanding of the adsorption system.

Funding by the DFG through SFB658 and TA244, and computing time within the DEISA Extreme Computing Initiative, is acknowledged. We thank J. Zegenhagen, Y. Mi, O. Neucheva, and S. Mohanty for support.

*s.tautz@fz-juelich.de

[1] Q. Wu and W. Yang, J. Chem. Phys. **116**, 515 (2002).
[2] S. Grimme, J. Comput. Chem. **25**, 1463 (2004).
[3] S. Grimme, J. Comput. Chem. **27**, 1787 (2006).
[4] P. Jurečka, J. Černý, P. Hobza, and D. Salahub, J. Comput. Chem. **28**, 555 (2007).
[5] N. Atodiresei, V. Caciuc, J.-H. Franke, and S. Blügel, Phys. Rev. B **78**, 045411 (2008); N. Atodiresei, V. Caciuc, P. Lazić, and S. Blügel, Phys. Rev. Lett. **102**, 136809 (2009).
[6] A. Tkatchenko and M. Scheffler, Phys. Rev. Lett. **102**, 073005 (2009).
[7] E. McNellis, J. Meyer, A. D. Baghi, and K. Reuter, Phys. Rev. B **80**, 035414 (2009); E. R. McNellis, J. Meyer, and K. Reuter, Phys. Rev. B **80**, 205414 (2009).
[8] A. Hauschild *et al.*, Phys. Rev. Lett. **94**, 036106 (2005).
[9] C. Stadler *et al.*, Phys. Rev. B **74**, 035404 (2006).
[10] A. Gerlach, S. Sellner, F. Schreiber, N. Koch, and J. Zegenhagen, Phys. Rev. B **75**, 045401 (2007).
[11] L. Kilian *et al.*, Phys. Rev. Lett. **100**, 136103 (2008).
[12] The fits were generated using the nondipolar parameters $Q = 0.22$, $\Delta = -0.26$ and $S_R = 1.89$, $S_I = 1.45$, $\Psi = -0.066$ for N1s and C1s, respectively [9,10].
[13] This intersection also defines the f_c of the C atoms which contribute to the vector sum; the spiral drawn in Fig. 1(d) already corresponds to the correct $f_c = 0.24$ that matches the experimental f_c at the intersection.
[14] S. Hagen, F. Leyssner, D. Nandi, M. Wolf, and P. Tegeder, Chem. Phys. Lett. **444**, 85 (2007); P. Tegeder *et al.*, Appl. Phys. A **88**, 465 (2007).
[15] K. W. Kolasinski, *Surface Science* (Wiley, West Sussex, 2001).
[16] S. Clark *et al.*, Z. Kristallogr. **220**, 567 (2005).
[17] J. P. Perdew, K. Burke, and M. Ernzerhof, Phys. Rev. Lett. **77**, 3865 (1996).
[18] M. Rohlfing and T. Bredow, Phys. Rev. Lett. **101**, 266106 (2008).